

Recent Developments and Future Projects at the ESRF

P. Berkvens

*European Synchrotron Radiation Facility
BP220
38043 Grenoble Cedex09
France
Email: berkvens@esrf.fr*

Abstract

The present paper describes some particular radiation protection issues of the phase I beamlines of the ESRF upgrade program. Since a number of these beamlines are long beamlines, the containment of the gas-bremsstrahlung has been verified, in particular under misalignment conditions. The paper also deals with one of the upgrade beamlines using white beam in all hutches. Finally one of the soft X-ray beamlines is described.

Introduction

Radiation protection design work at the ESRF since the Radsynch11 workshop was essentially concentrated on the phase I beamlines of the ESRF upgrade program. These upgrade beamlines include in particular 6 long beamlines which extend into the new experimental halls. For these long beamlines, misalignment conditions between the electron trajectory in the storage ring straight section and the front end / beamline axis must be looked at carefully to make sure that the gas-bremsstrahlung beam and the white synchrotron radiation beam will be contained under all conditions. Although the ESRF front end does not include lead bremsstrahlung collimators, we have clearly demonstrated that the different copper collimators provide an efficient collimator scheme for high energy bremsstrahlung photons (and by definition for synchrotron radiation). This is developed in more detail in the next paragraph.

During the last Radsynch11 workshop, we reported about the developments of the synchrotron radiation therapy programs on the ESRF medical beamline. In the meantime the formal authorisations from the French authorities have been obtained for the clinical program on human patients using the SSRT technique (Stereotactic Synchrotron Radiation Therapy). So far, 5 patients have been treated. Further progress has also been made concerning the MRT program (Microbeam Radiation Therapy). The first animal patients (dogs and cats with spontaneous tumours) are expected to be treated at the ESRF in November 2013.

Finally, ESRF is now actively preparing the phase II of its upgrade program. This includes the preparation of the Technical Design Report of the storage ring upgrade. From a radiation protection point of view this requires a full reassessment of the storage ring shielding as well as a detailed study of the decommissioning of the existing storage ring.

The rest of the present paper will deal with some specific radiation protection aspects of the phase I upgrade beamlines.

Transmission of gas-bremsstrahlung through the front end

The transmission of gas-bremsstrahlung through the ESRF standard front end, in particular under misalignment conditions, has been reassessed in view of the installation of a number of long beamlines in the framework of the phase I of the ESRF upgrade.

Four elements in the standard ESRF high-power front end are of importance in the definition of the gas-bremsstrahlung power transmitted through the front end into the beamline optics hutch. These elements are:

1. Collimator: installed at 13.06 m from the middle of the straight section, defining a 8 mm diameter circular aperture;

2. Horizontal slits: installed at 14.05 m from the middle of the straight section, defining a 2 mm full width, 30 mm full height rectangular aperture;
3. Movable absorber: installed at 14.59 m from the middle of the straight section, defining a 4 mm full width horizontal slit;
4. Vertical Slits: installed at 22.30 m from the middle of the straight section, defining a 30 mm full width, 4 mm full height rectangular aperture.

These elements are all made of (water cooled) copper. No lead collimators are foreseen in the front ends, other than the lead cladding of the port end wall. Although the copper thicknesses are not sufficient to completely stop the bremsstrahlung, they sufficiently scatter the bremsstrahlung cascades to obtain an efficient collimation, taking into account the length of the front end and the small solid angle defined by the port end vacuum vessel. This is illustrated in Figure 1, showing the gas-bremsstrahlung transmission through the front end.

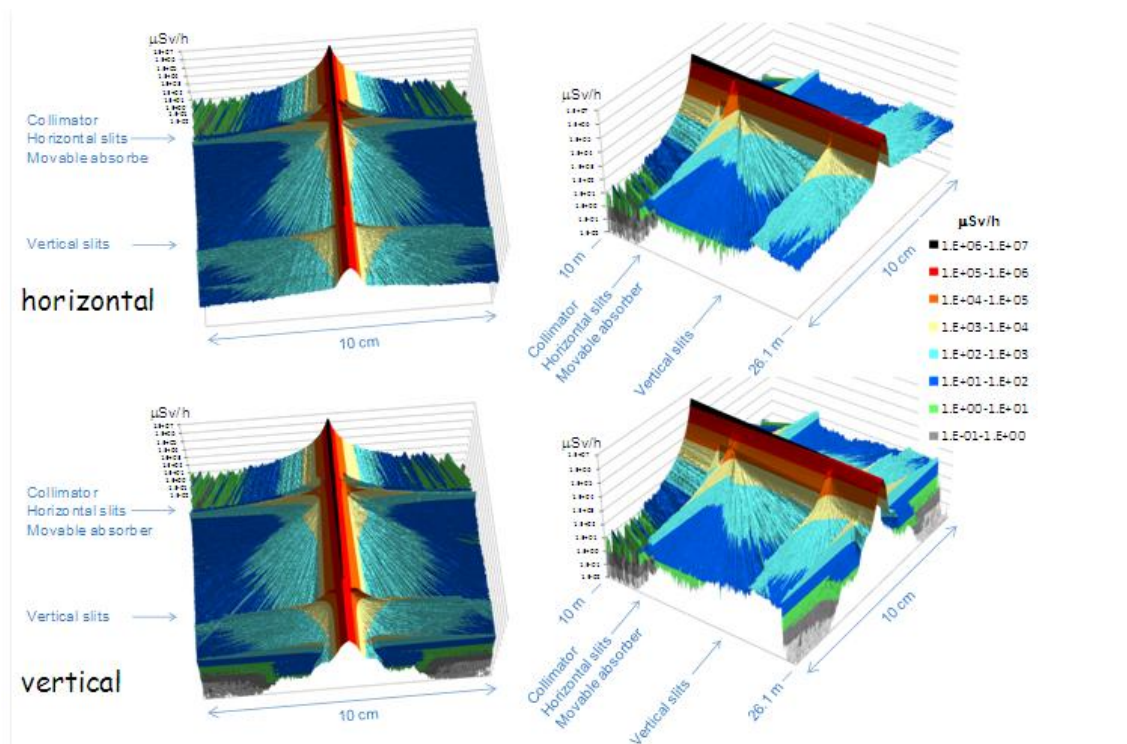


Figure 1 - Gas-bremsstrahlung transmission through the front end. - Top: ambient dose equivalent distribution in a horizontal plane (full vertical scoring height = 2 mm) – Bottom: ambient dose equivalent distribution in a vertical plane (full horizontal scoring width = 2 mm). Beam conditions: 200 mA, $1 \cdot 10^{-9}$ mbar average pressure in straight section.

The efficiency of the copper collimators is further illustrated in Figure 2, showing the gas-bremsstrahlung transmission through the front end in case of horizontal misalignment between the electron beam in the straight section and the front end (angular misalignment combined with a horizontal offset to keep 100 % transmission through the horizontal slits).

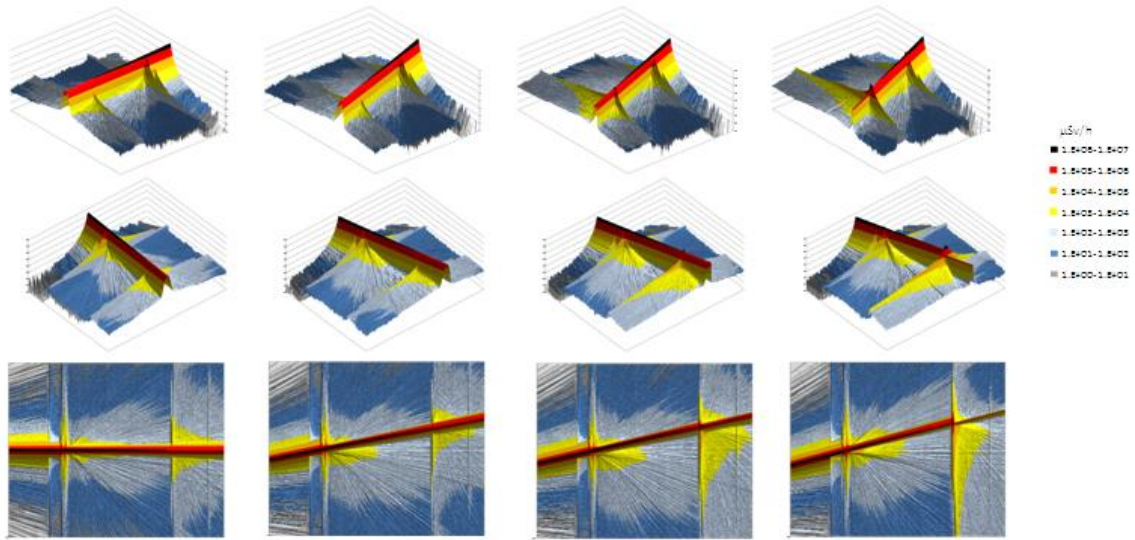


Figure 2 - Gas-bremsstrahlung transmission through the front end in case of horizontal misalignment between the electron beam in the straight section and the front end: dose equivalent distribution in a horizontal plane (horizontal scale: from 10 to 26.12 m from middle of straight section; vertical scale: ± 5 cm around theoretical front end beam axis; full vertical scoring height = 2 mm) – From left to right: misalignment angle = 0 mrad, 1.5 mrad, 1.75 mrad, 2 mrad.

One clearly sees that the gas-bremsstrahlung beam gets clipped for horizontal misalignment angles above 1.75 mrad. The collimating effect of the first optical elements in the optics enclosures of a typical beamline will be even more pronounced, as these first elements are typically high-power slits or fixed apertures. This is illustrated in Figure 3, showing the effective dose rate distribution in the first part of the UPBL01/ID01 optics hutch, for increasing horizontal misalignment angles between the electron beam and the front end. One sees that for misalignment angles above 0.25 mrad, the gas-bremsstrahlung is completely stopped in the (copper) body of the high-power slits.

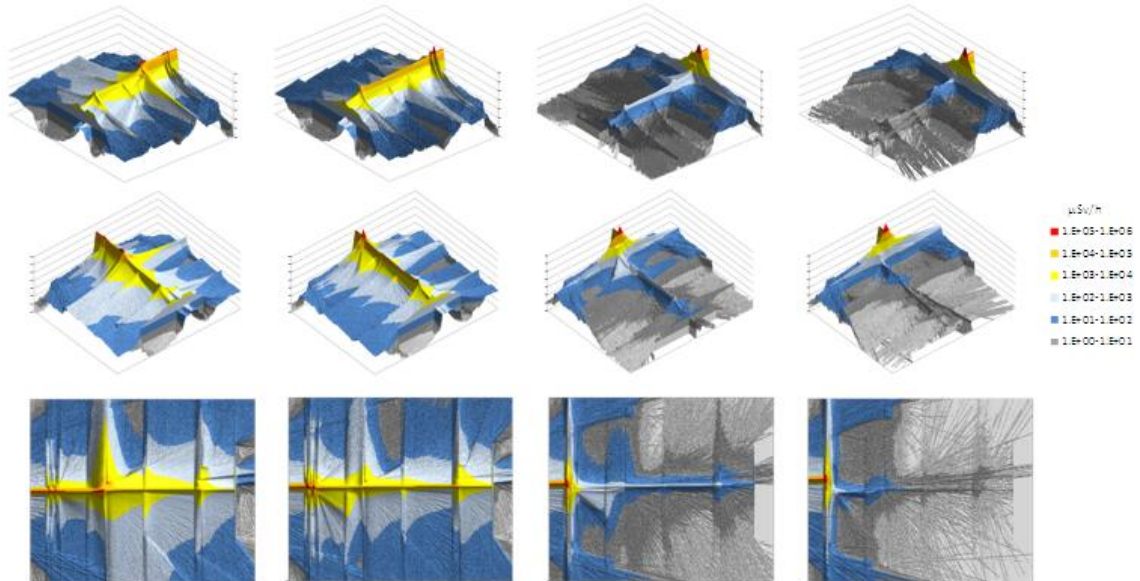


Figure 3 - Effective dose rate distribution in the first part of the UPBL01/ID01 optics hutch. Dose distribution in horizontal plane at beam height: x: 0 – 1100 cm; y: -10 – 10 cm; total vertical scoring height = 2 cm – Beamline configuration: high power slits: horizontal half width = 1.5 mm, vertical half height = 1.5 mm – 1st mirror: 6 mrad – 2nd mirror: 6 mrad, 1.2 cm offset – Horizontal secondary slits: half opening 1.25 cm – Vertical secondary slits: half opening 0.25 cm – Multilayer monochromator: 0.01716 mrad, 1.37 cm offset. From left to right: misalignment angle = 0 mrad, 0.25 mrad, 0.5 mrad, 1 mrad.

The UPBL2 / ID31 beamline

The UPBL2/ID31 high energy beamline for buried interface structures and materials processing is for the time being the only beamline with white beam hutchches inside the new experimental halls.

The parameters of the insertion device are given in Table 1, corresponding to the use of two 2-meters long cryogenic undulators at minimum gap.

Period	14 mm
Length	4 m
Magnetic field	1.2 T

Table 1 – Insertion device parameters used for the calculations.

The ID13 beamline will use a non-standard design by the incorporation of two extra fixed slits, defining a 1 mm × 1mm beam aperture. The slits are located behind the standard front end vertical slits, between 23.18 and 23.5 meters from the middle of the straight section, and therefore correspond to a $43 \times 43 \mu\text{rad}^2$ aperture. Figure 4 shows the effective dose rate distribution in a vertical plane along the ID31 front end, from 10 meters from the middle of the straight section to 26.12 m from the middle of the straight section, corresponding to the external face of the port end wall. One clearly sees the collimating effect of the different slits, in particular of the specific ID31 1 mm² slits.

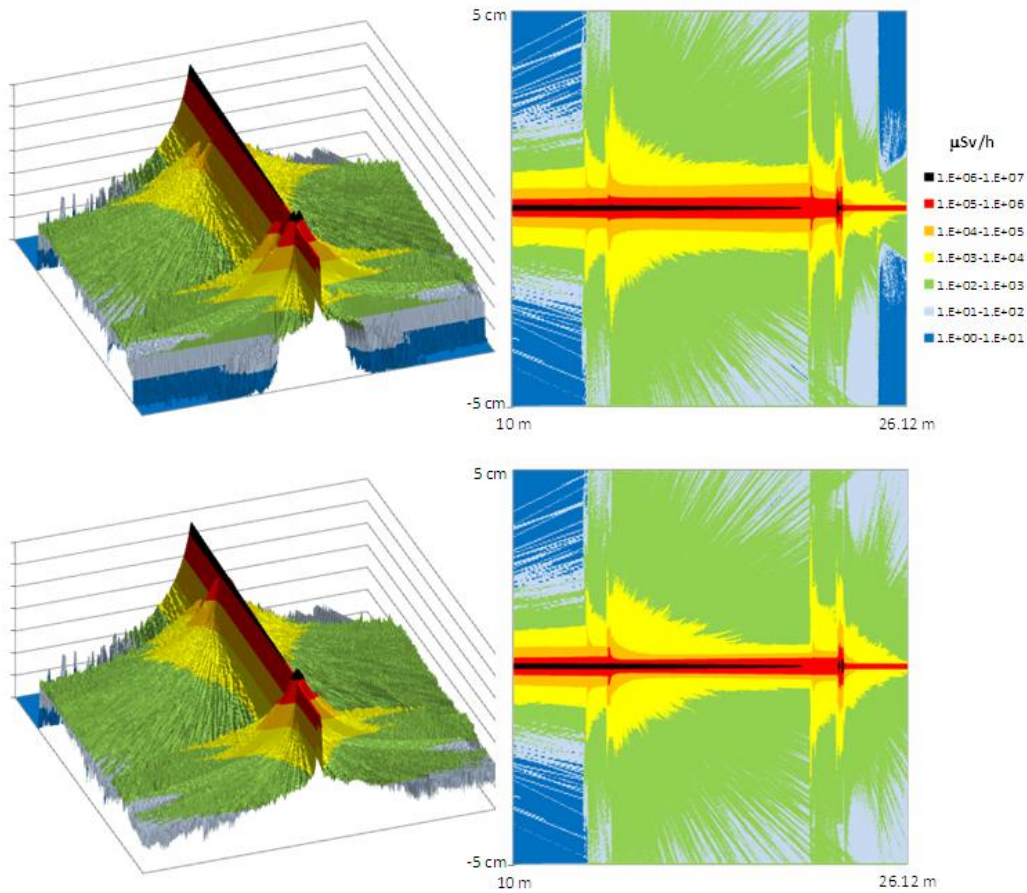


Figure 4 - Gas-bremsstrahlung transmission through the ID31 front end. Top: ambient dose equivalent distribution in a vertical plane (full horizontal scoring width = 2 mm) – Bottom: ambient dose equivalent distribution in a horizontal plane (full vertical scoring height = 2 mm).

Due to the efficient collimation of the gas-bremsstrahlung, the shielding requirements of the white beam hutches will be determined by synchrotron radiation. This is illustrated in Figure 5.

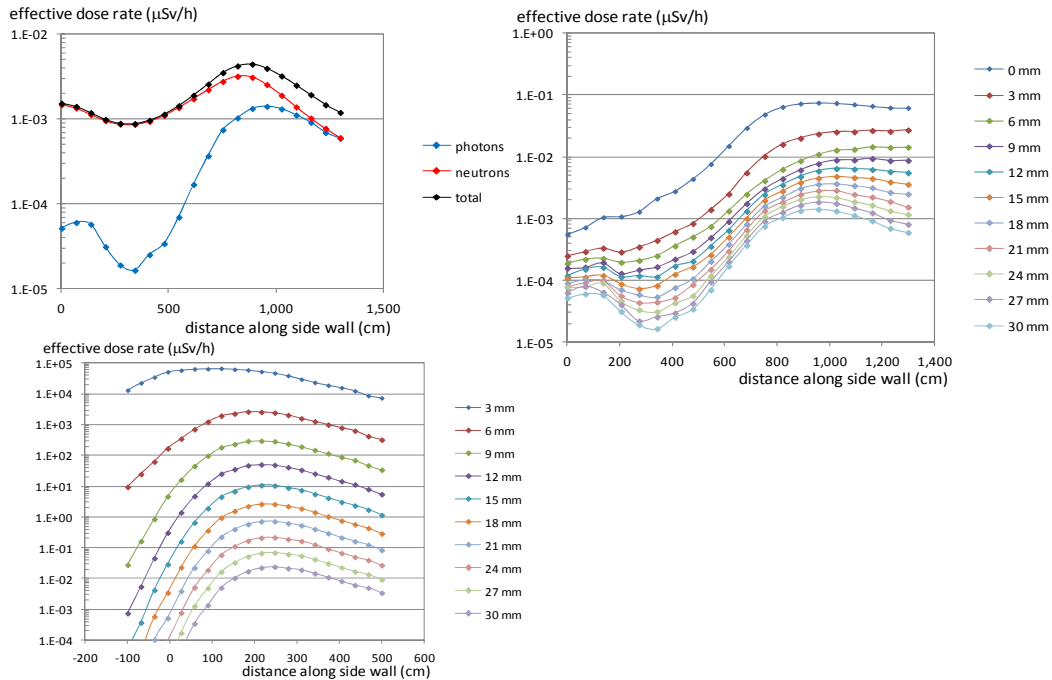


Figure 5 – Shielding calculations for the side walls of the OH2 optics hutche. Top right: effective dose rate behind side wall for scattered gas-bremsstrahlung as a function of the distance along the side wall for different values of the lead thickness. Top left: scattered gas-bremsstrahlung and photo-neutron effective dose rates behind the 30 mm thick side wall, as a function of the distance along the side wall. Bottom: effective dose rate behind side wall for scattered synchrotron radiation as a function of the distance along the side wall for different values of the lead thickness.

The temperature stability requirements inside the OH2 and EH1 hutches of the UPBL02/ID31 beamline imply the installation of large air entrance and air exhaust chicanes on these hutches. The large transverse dimension of these chicanes and the fact that white beam is used inside the hutches has made a more detailed shielding study of these chicanes necessary. Figure 6 shows the layout of the ID31 OH2 and EH1 hutches with the position of the 4 air entrance chicanes on the roof. A 2 mm steel lining is foreseen inside the lead chicanes.

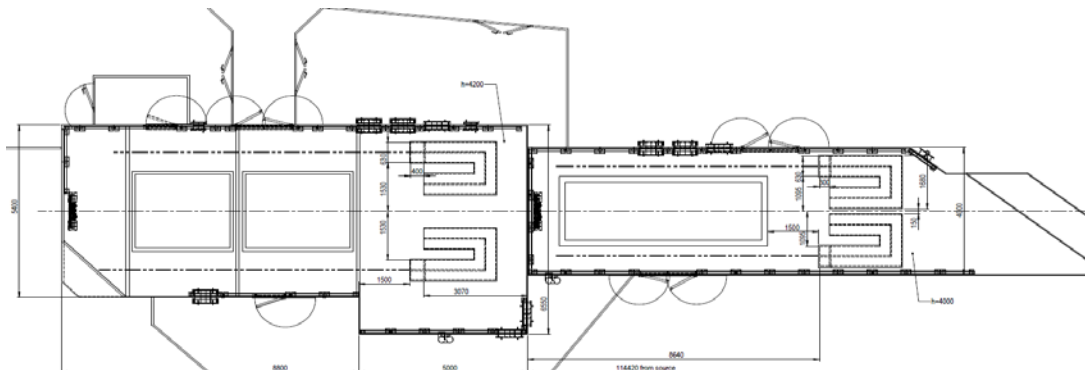


Figure 6 – Layout of the ID31 OH2 and EH1 hutches with the position of the 4 air entrance chicanes on the roof.

Figure 7 shows the geometry of the two identical air entrance chicanes of the second optics hutch. Each chicane consists actually of two independent chicanes, with a cross-sectional surface of $30 \times 30 \text{ cm}^2$. From a radiation protection point of view, the "inner" chicane, with the shortest second leg, will be the most constraining. For the calculations we therefore concentrate on this inner chicane.

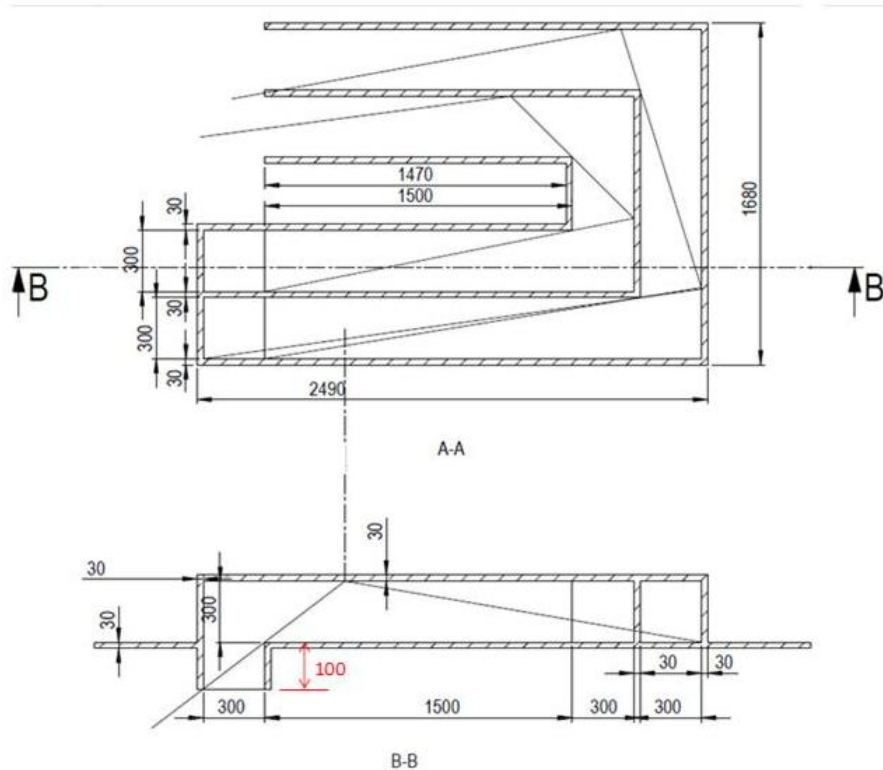


Figure 7 – Geometry of the air entrance chicanes in the second optics hutch.

We assume a low-Z (silicon) grazing incidence scatter (no self absorption) as a primary scattering source to define the radiation entering the chicane. We consider a scattering source which is located at 2 m upstream of the chicane entrance mouth (see Figure 8).

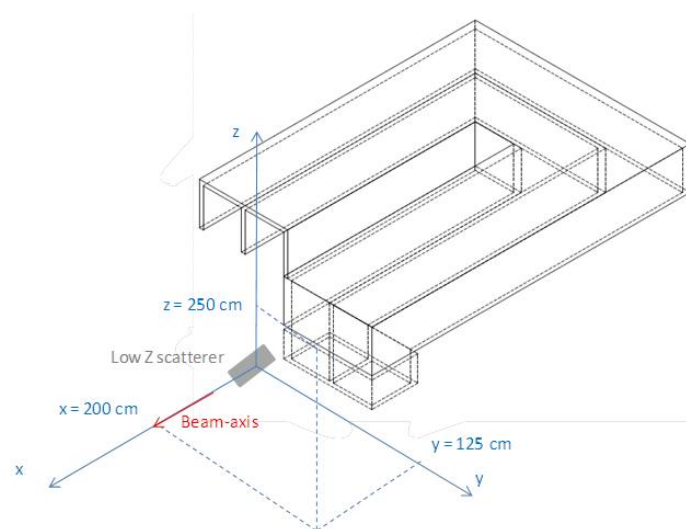


Figure 8 – Scattering geometry used for characterisation of the OH2 air entrance chicanes. The entrance mouth of the chicane is located at $x = 200 \text{ cm}$, $y = 125 \text{ cm}$ and $z = 250 \text{ cm}$ relative to the scattering source.

Figure 9 shows the differential photon fluence at different positions through the chicane, respectively at the entrance mouth, at the end of the 1st leg of the chicane, at the end of the 2nd leg of the chicane and at the exit mouth of the chicane. One sees that the photon intensity at the exit of the chicane is reduced by more than 10 orders of magnitude relative to the intensity at the entrance of the chicane.

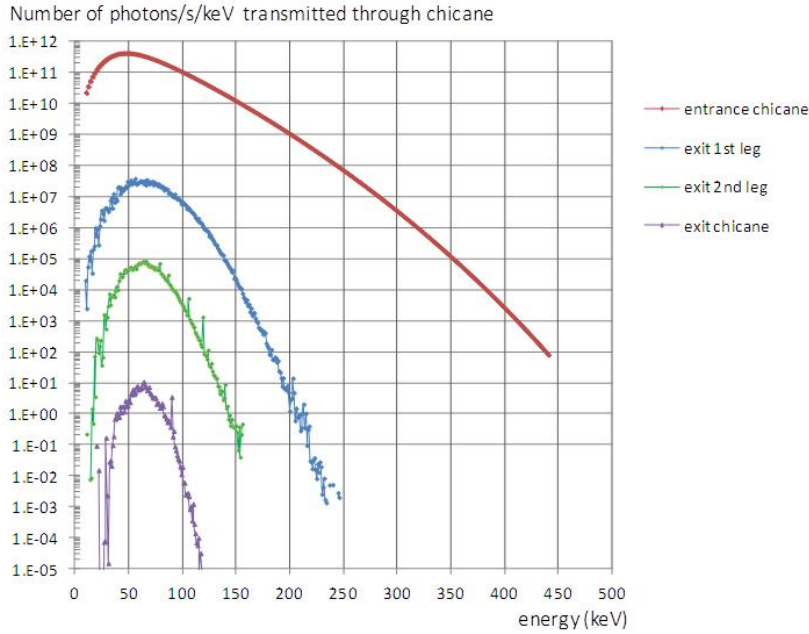


Figure 9 – Differential photon fluence at different positions through the chicane, respectively at the entrance mouth, at the end of the 1st leg of the chicane, at the end of the 2nd leg of the chicane and at the exit mouth of the chicane.

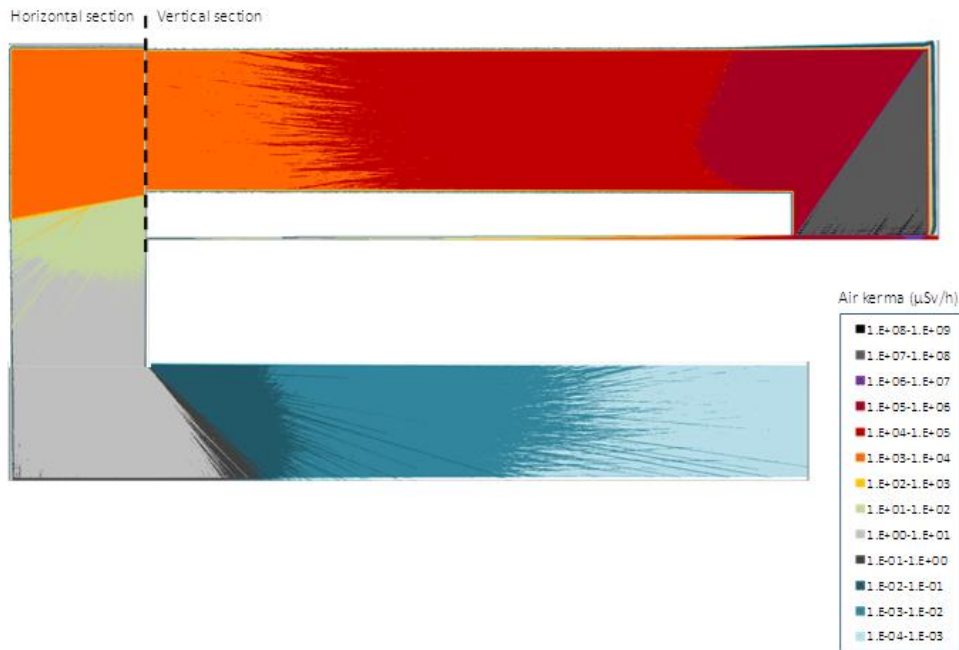


Figure 10 – Air kerma distribution through the chicane, showing, for a given position, the average value over the entire chicane cross-sectional surface. The first leg corresponds to a vertical section, the second and third leg to a horizontal section.

The effect of the chicane is further illustrated in Figure 10, showing the air kerma distribution through the chicane, showing, for a given position, the average value over the entire chicane cross-sectional surface. The first leg corresponds to a vertical section, the second and third leg to a horizontal section. One sees that the dose rates at the exit of the chicane are reduced to values well below natural background.

The UPBL7/ID32 beamline

The UPBL7/ID32 soft X-ray beamline for magnetic and electronic spectroscopy is one of only two beamlines at the ESRF where, due to the low energy of the X-rays, no further lead hutches are foreseen downstream of the optics hutch. This can only be achieved if an efficient collimation system for scattered gas-bremsstrahlung and Compton-scattered synchrotron radiation is foreseen inside the optics hutch. In the case of UPBL7/ID32, this collimation is obtained via

1. A 14 cm thick, 7.5 cm diameter tungsten block, installed in a dedicated vessel behind the double mirror vessel, with a $10 \text{ mm}_H \times 6 \text{ mm}_V$ beam opening.
2. Two 5 cm thick tungsten collimators, with $10 \text{ mm}_H \times 6 \text{ mm}_V$ beam openings, installed respectively at the beginning and at the middle of the 2 meter long lead collimator at the end of the optics hutch.

Figure 11 shows the effective dose distribution in a horizontal plane throughout the ID32 optics hutch, respectively for gas-bremsstrahlung, photo-neutrons and synchrotron radiation, showing that the radiation levels, due to the different types of scattered radiation, behind the optics hutch will be sufficiently attenuated.

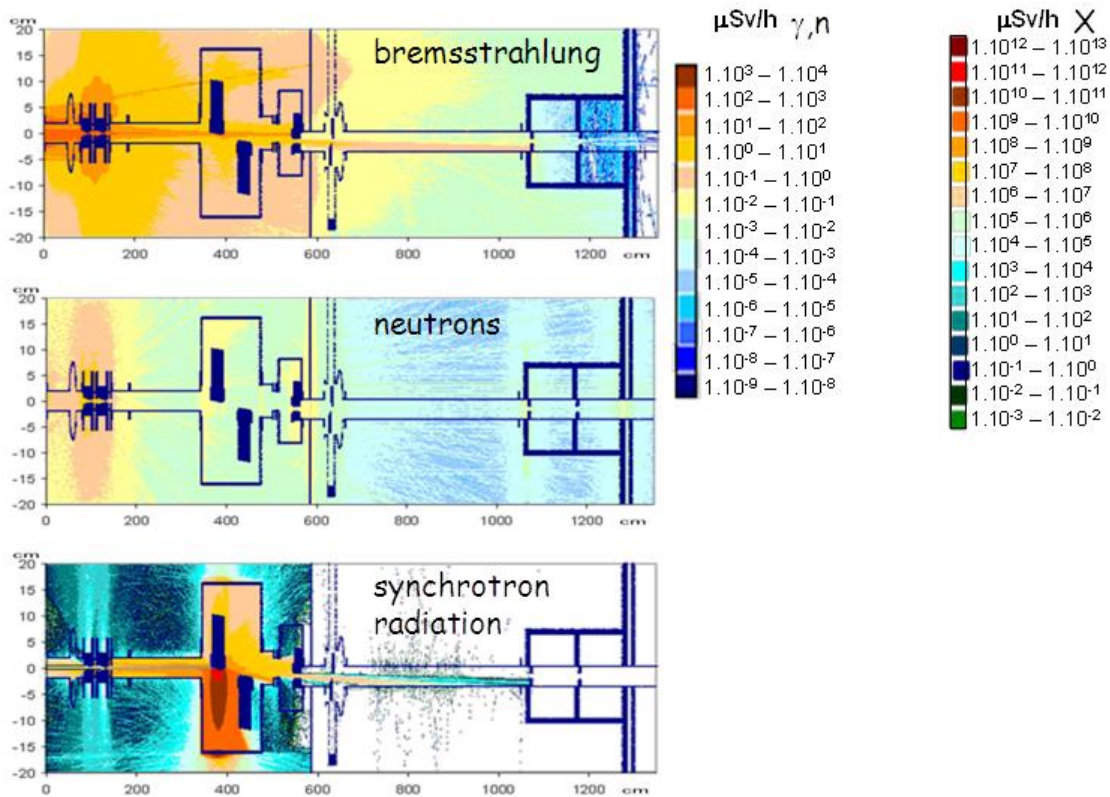


Figure 11 – Effective dose distribution in an horizontal plane (scoring height = 2 mm) throughout the ID31 optics hutch. Top: gas-bremsstrahlung. Middle: photo-neutrons. Bottom: synchrotron radiation.